Sambo, S.N., Hockaday, C.S.A., Seodigeng, T., 2020. The Development of a Heat and Mass Transfer Model for a Shaft Kiln to Preheat Manganese Ore with Hot Air, Model Development Methodology, in: Peng, Z., Hwang, J.-Y., Downey, J.P., Gregurek, D., Zhao, B., Yücel, O., Keskinkilic, E., Jiang, T., White, J.F., Mahmoud, M.M. (Eds.), 11th International Symposium on High-Temperature Metallurgical Processing, The Minerals, Metals & Materials Series. Springer International Publishing, Cham, pp. 43-53. https://doi.org/10.1007/978-3-030-36540-0_5

The development of a heat and mass transfer model for a shaft kiln to preheat manganese ore with hot air, model development methodology

Sifiso N. Sambo[1], Carolina S.A Hockaday[2], and Tumisang Seodigeng[3]

[1&2] MINTEK, Johannesburg, South Africa. 200 Malibongwe Drive, Randburg, 2194.

sifisos@mintek.co.za/ linah@mintek.co.za, +27 (0)11 709 4694

[3] Vaal University of Technology, Vanderbijlpark, South Africa. Andries Potgieter Blvd, Vanderbijlpark, 1900

tumisangs@vut.ac.za, +27 (0)16 950 9655

Abstract: This work models the design of a preheater (shaft kiln) to demonstrate preheating of manganese ores with hot air at 800°C produced by concentrating solar thermal energy on a pilot scale. This paper report the methodology for the development of a heat and mass transfer model that informs the effective control of the shaft kiln air flow rates. A continuum approach is followed through the discretisation of the fluid and solid phases of a packed bed of randomly packed lumpy mineral ore. The fluid dynamics of the packed bed is solved using correlations for fluid flow through packed beds and the dimensionless constants for flow, heat convection and conduction are quantified for a packed bed of manganese ore. The required pressure drop across the shaft kiln with fluid flow up to 5 m/s is less than 100 kPa. It was also found that a lumped system does not exist in the solid phase. The validity of the model will be studied theoretically and through experimental work. Outstanding work on the methodology include the solution to the radiative heat transfer, convective mass transfer, and the method to measure the extent at which the wall effect have on the radial temperature distribution.

Keywords: Shaft kiln; Packed bed; Heat and mass transfer; Convection; Radiation; Conduction

1. Introduction

This research study models a shaft kiln with packed manganese ore where air is used for thermal energy transfer in the fluid-solid interface. This is part of on-going studies on the implementation of concentrated solar thermal energy in minerals processing to eliminate the burning of fossil fuels. If commercialized, this will be the first application of concentrated solar thermal energy for high temperatures above 400 °C [1]. Heating manganese ore up to 600 °C in oxidizing environment decompose carbonate minerals and vaporize hydroxides [2] which reduce the amount of carbon monoxide and water vapor released during smelting in a submerged arc furnace to save furnace power consumption.

Packed beds provide a high surface area to volume ratio [3], and give effective heat and mass transfer between fluid and solids in various unit operations. This work studies the heat transfer process from the fluid (air) to the solids (Mn ore) and the mass transfer from Mn ore to the fluid phase in the shaft kiln. Several studies [3, 4, 5] have developed heat and mass transfer models for packed beds with fluid to solid heat transfer. The influence of material and fluid properties, packing arrangement, and fluid dynamics has appeared to play an important role in these fluid-solid heat transfer models. Packing structural arrangement is one of the first fundamentals that need to be understood before an analysis on heat transfer can be carried out. This is because the characterization of the fluid-solid medium interface is the defining factor of the transfer process rather than the thermo-physical property of the bed [6].

The column wall affects the geometry of the packing structure both in the radial and axial direction. This results in existing temperature gradients in the radial direction due to fluid channelling at the wall surface [7]. The wall effect extends to five particle diameter in both directions but the axial effect is generally negligible due to the column height [6]. The axial temperature gradients exist due to the fluid-solid heat transfer up the column. The axial and radial thermal conductivity contribute to the overall heat transfer coefficient and a two dimensional axial dispersion (2DADPF) model [8] presents the general energy balance for a plug flow model which include both the axial and radial bed conductivity as Equation 1, and the boundary condition applied at the wall as Equation 2.

$$GC_f \frac{\partial T}{\partial x} = k_{er} \frac{\partial}{r\partial r}\left(r \frac{\partial T}{\partial r}\right) + k_{eax} \frac{\partial^2 T}{\partial x^2} \quad (1)$$

$$k_{er} \frac{\partial T}{\partial r} = h_w (T_f - T_w) \quad (2)$$

G (kg/s) is the fluid mass flux in the axial direction, C_f (J/g.K) is the fluid heat capacity, T_f and T_w are the fluid temperature and bed temperature respectively, k_{er} and k_{eax} (W/m.k) are the radial and axial bed thermal conductivities.

The continuum approach to heat and mass transfer modeling of randomly packed beds made up of randomly shaped lumpy mineral ores in fluid-solid transport systems requires a proper fluid dynamic model. This is because the fluid dynamics governs the heat transfer in the fluid-solid interface. This problem becomes more complex because of the random flow pattern and the mixing of the fluid in the void regions. In principle, the governing Navier Stokes equations of flow must be applied [4]. The application of the Navier Stokes equations requires well defined boundary conditions for all the particles in the packed bed which complicate the solution to the fluid dynamics problem. Computational discretization allows for the description of the packed bed as an assembly of discrete particles and provides a solution for the fluid flow problem. However, the elementary approach (DEM) requires sophisticated algorithms and high computational power. The continuum approach is simplified in this work and the fluid flow problem is solved using the experimentally derived correlations of fluid flow in packed beds.

2. Methodology

2.1. Approach to packed bed modelling

The fluid stream pressure drop is the driving force that ensures the flow of air through the packed Mn ore up in a shaft kiln. The flow parameters are studied by first defining the flow regime and relating the pressure drop to the fluid flow velocity using empirical correlations of flow through packed beds. In principle, packed beds of solid material of uniform particle size (D_p) distribution have an equal surface area per unit volume. This allows for the discretization of the fluid-solid interfaces as a bundle of tubes within the column cross sectional area. The fluid tube's equivalent diameter (D_{eq}) and the bed void fraction determine how many such tubes (n) occupy the given column cross sectional area (S_o). The visualization of the packed bed model can be seen in Figure 1 (a) and (b). Due to the fluid flow pattern, the model length (ΔL_m) is less than the actual flow length. However, this is corrected by a constant value determined by applying the empirical correlations for flow through packed beds.

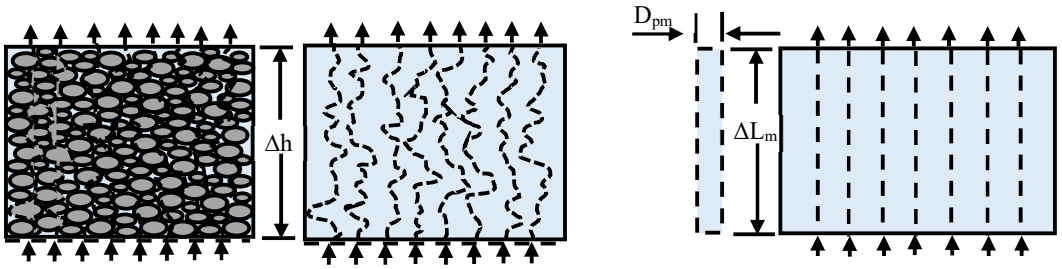

Figure 1: a) Actual packed bed of length ΔL b) Packed bed model of length ΔL_m

To define the Mn ore packed bed geometry, assumptions of the shaft kiln dimensions and the characterization of Mn ore size distribution is required. The lumpy Mn ore particle size distribution (Dp) have shown that particles size bigger than 20 mm contribute over 80% of the Mn ore sample total mass. However, in this work we consider the particles size of 5.6 – 20 mm. An internal report on characterization of the UMK Mn ores have shown equal distribution of minerals composition across all size fractions and this makes it possible to select the desired size fraction. The small size fraction gives some tolerance for the porosity variation in the radial direction in small scale columns. To characterize the packed bed as a bed of uniform size particles, the mean particle diameter (D_{pm}) was determined based on the particles size distribution presented in Table 1.

Table 1: Mean particle diameter

Dp range (mm)	Dp intervals (mm)	Cumulative mass (kg)	Weight fraction (x)	$(x/D_p)_i$
5.6-10.0	7.8	35	0.201	0.0258
10.0-16.0	13	95	0.345	0.0265
16.0-20.0	18	174	0.454	0.0252
		Sum $(x/D_p)_i$		0.0775
		Mean particle diameter $= 1/(x/D_p)_i$		12.897

The lumpy Mn ore was characterized as broken solids and the value of sphericity was adopted from Kunni and Lavenspiel [9] as 0.63. A 200 mm column diameter (D) and 1200 mm height is used in this work. A column of similar dimensions will be used for the lab experimental work to validate the model. The Buckingham Pi theorem and similitudes will be used to scale for larger applications. The packed bed properties specified above allows for the evaluation of porosity variations across the packed column but the packed bed average porosity was used for simplicity. The average bed porosity of the Mn ore was evaluated in the laboratory using fluid displacement method and was found to be 0.48. The column cross sectional area is related to the solid phase and the fluid phase tubes by Equation 3 & 4 and the two equations equate to solve for the equivalent diameter, Equation 5. The actual fluid flow velocity (V) is related to the superficial velocity (V_0) and the porosity (ε) as shown in Equation 6. This equation is employed for the evaluation of convection heat and mass transfer parameters in the fluid-solid interphase. For the given bed porosity, particle mean diameters (D_{pm}) and sphericity (Φ_s), and the bed total surface area (S_0), the fluid tubes equivalent diameter was found to be 8.03 mm and 298 fluid phase tubes.

$$n(\pi D_{pm}\Delta L) = S_0\Delta L(1-\varepsilon)\left(\frac{6}{\Phi_s D_{pm}}\right) \quad (3)$$

$$n\left(\frac{1}{4}\pi D_{eq}^2\right)\Delta L = S_0\Delta L\varepsilon \quad (4)$$

$$D_{eq} = \sqrt{\frac{2\times D_{pm}^2\times \Phi_s}{3}\times\frac{\varepsilon}{(1-\varepsilon)}} \quad (5)$$

$$V = \frac{V_0}{\varepsilon} \quad (6)$$

2.2. Convective heat transfer

The arrangement of the fluid-solid interface as a bundle of tubes simplifies the bed characterisation and the heat transfer problem but does not give the correct dimensionless constants for fluid flow parameters. The pressure drop per unit length to the fluid flow superficial velocity for flow in packed beds at low Reynolds numbers, (R_{ep} < 2300) is given by the Kozeny Carmen correlation [9]. At high Reynolds numbers (R_{ep} > 2300) the effect of the friction factor becomes low ($f \rightarrow$ constant) and the pressure drop is evaluated using the Burke Plummer equation [9]. The correlations enable the assumptions of the fluid velocity given the required pressure drop across the length of the packed bed. This means that a fully developed velocity profile can be assumed and the convective heat transfer governing equations can be evaluated. Both the Kozeny Carmen and the Burke Plummer equations combine to form the Ergun equation which is used to solve problems where the flow is transitional, however one term always dominates depending on the R_{ep} values [9].

The value of the measured Mn ore packed bed average porosity is high (0.48) for randomly shaped particles compared to spherical particles of the same size. This is caused by the low sphericity values for non-spherical materials. Empirical correlations for porosity values of spherical particles (Φ=1) relate the particles diameter to

the column diameter as presented in Equation 7 [6, 8]. The required pressure drop across the bed of lumpy Mn ore is expected to be lower due to high porosity. However, for the same Reynolds number the friction factor is high due to low sphericity of the Mn ore particles. The friction factor was evaluated using Equation 8 and the results were plotted against the values of R_{ep} at a log scale in Figure 2. It can be seen from figure 2 that the friction factor becomes a constant at high R_{ep} values which shows the transition from laminar to turbulent flow. All values of the fluid properties, density (ρ) and viscosity (μ) used were taken at a bulk mean temperature assuming that 80 % of the fluid temperature (800 °C) is lost to the solid phase in the column. The fluid delivery pressure of 250 kPa was used. Figure 3 below shows the relationship between fluid superficial velocity and pressure drop for both lumpy Mn ore and spherical Mn ore of the same size.

$$\varepsilon = 0.375 + 0.34 \times \left(\frac{D}{D_p}\right) \quad f_{bed} \tag{7}$$

$$f_{bed} = \frac{150}{\Phi_s^2 \, R_{ep}} + \frac{1{,}75}{\Phi_s} \tag{8}$$

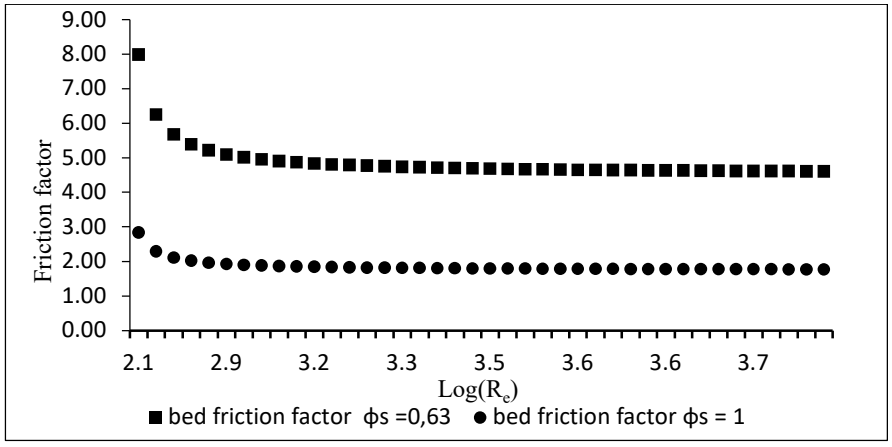

Figure 2: Friction factor against log scale R_{ep} values for spherical and lumpy Mn ore

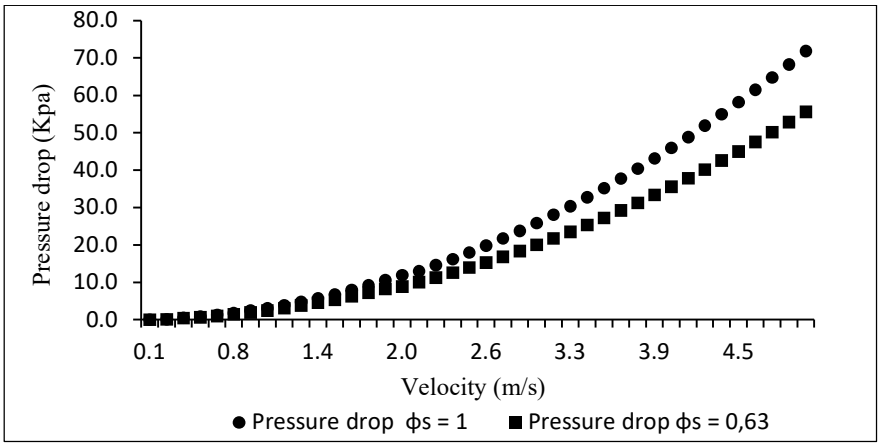

Figure 3: Pressure drop against superficial velocity

The packed bed heat transfer coefficient will be evaluated with dimensionless numbers at an entry region until fully developed temperature profiles are established. When the whole packed bed is a fully developed region the local heat transfer coefficient and the temperature gradients across the bed length remains the same. Parameters of the entry region determines the start-up time before a continuous flow of the Mn ore stream to ensure that the furnace feed is at the required temperature of 600 °C. Hot air (800 ˚C) will be supplied at a constant rate to heat

the solids which are at a lower temperature; this means that a constant wall heat flux arrangement can be assumed given that the bed is made up of material with constant thermal conductivity (k), specific heat capacity (C_p), and thermal diffusivity (α). All Mn ore thermo-physical properties will be evaluated at the bulk mean temperature. Assuming that the velocity profile is fully developed, the heat transfer coefficient (h) will be evaluated using the dimensionless Nusselt number over a length L. For the thermal entrance region, N_{uDL} is evaluated as a function of a dimensionless axial distance (L^*) given by Equation 10 and used in Equation 9. Two empirical correlations that relates N_{uD} and L^* with limits to the values of L^* are presented in Equation 11 & 12. R_{eD} (Equation 13) is the dimensionless Reynolds number evaluated based on the flow path equivalent diameter (D_{eq}) and the fluid viscosity (μ). The dimensionless Prandlt number (P_r) can be obtained using Equation 14 and was taken to be 1 for air. Values of the Nusselt number based on the characteristic length were evaluated for the given packed bed properties and 1.56 m/s actual fluid velocity and plotted against the column length (ΔL) in Figure 4. It can be seen that N_{uD} values decreases across the column length which indicates that the thermal resistance increases up the column. This indicate that constant temperature profiles have not been established across the column.

$$N_{uD} = \frac{hL}{K} \tag{9}$$

$$L^* = \frac{\left(\frac{L}{D}\right)}{R_{eD}P_r} \tag{10}$$

$$N_{uD} = 1.953(L^*)^{\frac{1}{3}} \qquad for\ L^* < 0.03 \tag{11}$$

$$N_{uD} = 4.364 + \frac{0.0722}{L^*} \qquad for\ L^* \geq 0.03 \tag{12}$$

$$R_{eD} = \frac{\rho V D_{eq}}{\mu} \tag{13}$$

$$P_r = \frac{C_p \mu}{K}, \qquad \approx 1 \tag{14}$$

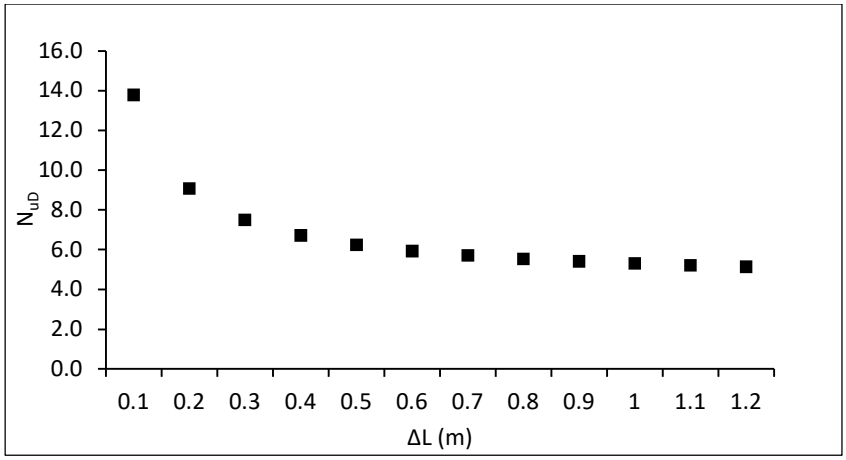

Figure 4: Nusselt number reduction with column length

When fully developed temperature profiles are established the flow of materials down the column can be assumed. This calls for the evaluation of the fully developed temperature profiles in axial segments of length L, that is, the temperature profile ($T_n - T_{n+1}$) of a given tube segment must remain the same when the solid materials flow down the column. This means Mn ore at a constant temperature will exit the column. If this is achieved the residence time of the materials in the column can be realized and controlled based on the thermal transport processes that take place. At this point the mathematical definition of temperature as a function of the tube radius (r), the length (L), and a constant (C_1) that relates the temperature distribution to the constant wall heat flux ($-q/A$), can be

employed (Equation 15) and the general energy equation for laminar flow in a tube of constant properties can be reduced to Equation 16.

$$T = f(r) + C_1 L \tag{15}$$

$$\frac{d}{dr}\left(r\frac{dT}{dr}\right) = \frac{C_1}{\alpha} r V_L = \frac{C_1}{\alpha} r V_{max}(1 - \frac{R^2}{R^2}$$
$$at\ r = 0: \frac{dT}{dr} = 0\ ;\ at\ r = R(tube\ wall):\ K\frac{dT}{dr} = \left(\frac{q}{A}\right)_w \tag{16}$$

The above correlations of convective heat transfer are only applicable for laminar flow of the fluid through the packed bed. The effect of the boundary conditions and the thermal entry length becomes small at high Reynolds numbers [10]. For fully developed velocity and temperature profiles the local heat transfer coefficient in the Nusselt number format can be evaluated using the Dittus-Boelter correlation [10, 11] in Equation 17. This correlation holds true for $0.3 < P_r < 100$, and $2300 < R_{eD} < 1.2x10^5$. A linear relationship exist between the Nusselt number and the Reynolds number for the packed Mn ore under fully developed velocity and temperature profiles. The relationship was evaluated for turbulent flow and the Reynolds number was plotted against the heat transfer coefficient in Figure 5.

$$N_{uD} = 0.023 \times R_{eD}^{0.8} \times P_r^{0.4} \tag{17}$$

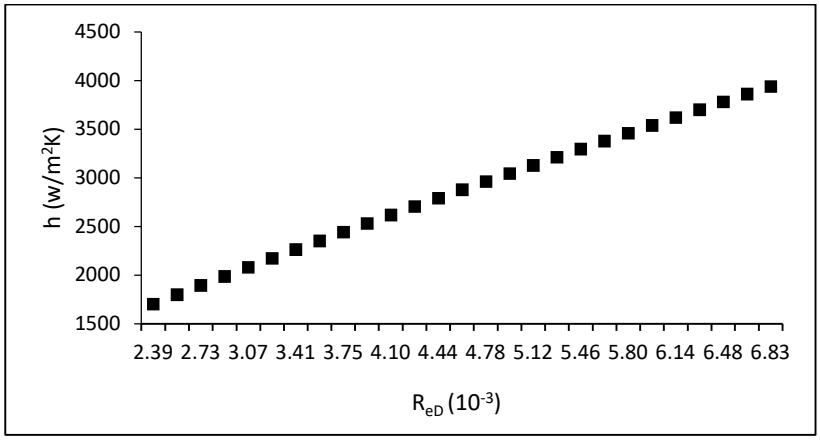

Figure 5: The fluid phase heat transfer coefficients for different values of R_{eD}

2.3. Conduction heat transfer

To study the conduction heat transfer the focus switches to the solid phase of the packed bed. An infinitely long cylinder of diameter D_{pm} subjected to the fluid phase temperature T_f was considered. Equation 19 gives the unsteady state conduction general differential equation on a one dimensional coordinate system neglecting the heat generation term. Heat generation is negligible because the decomposition reactions of the carbonate minerals in the Mn ore take place at temperatures above 650

$$K\frac{\partial^2 T}{\partial x^2} = \rho C_p \frac{\partial T}{\partial t} \tag{19}$$

Where C_p is the specific heat capacity of the solid materials.

For the given particle size distribution, the significance of internal temperature gradients were evaluated using the dimensionless Biot number (B_i) [10] which takes into account the convective thermal resistance at the surface of the solid materials. The value of B_i is given by the ratio of the product of the thermal resistance to convection at the surface (h) and the characteristic length (R) of the material to the internal thermal resistance (k). Values of $B_i > 0.1$ indicate that significant temperature gradients exist for the characteristic length of the solid material when

exposed to the fluid which is at high temperature [10, 11]. The thermo-physical properties of the Mn ore (C_p and α) were analysed using the laser flesh method using an LFA 457 Microflash at a 100 ˚C increments. The values of thermal conductivity were calculated for each temperature using Equation 20. The analysis results are presented in table 2 below, adopted from PreMa internal report D3.1.

$$k(T) = \alpha(T)Cp(T)\rho(T) \quad 20$$

Table 2: Thermo-physical properties of UMK Mn ore

T (˚C)	α (mm^2/s)	Cp (J/gK)	k (W/mK)
100	0.717	0.846	2.33
200	0.620	0.927	2.20
300	0.548	0.937	1.96
400	0.493	0.976	1.87
500	0.451	0.991	1.68
600	0.402	0.985	1.49
700	0.339	0.886	1.12
800	0.279	0.765	0.79

The B_i number for the cylindrical slab (D_{pm}) evaluated on the fluid bulk mean temperature and the fluid thermal resistance (h) have given values above 4. To quantify the temperature gradients a solution can be obtained by solving for both the length and the time differential terms in the unsteady state conduction general differential equation (19). The solution to temperature distribution will be obtained as a function of the dimensionless measure of time (Fourier number (F_u)), Dimensionless measure of location (Δr/R), and the Biot number. The temperature distribution results are presented graphically using chart that presents the temperature history at the centre of an infinitely long cylinder and the ratio of the temperature at any point in an infinitely long cylinder to the temperature at the centre line. [10, 11] covered chapters on unsteady state conduction and presented the product solution in Equation 21.

$$\frac{\theta}{\theta_0} = \left(\frac{\theta r_{/R=0}}{\theta_0}\right) \times \left(\frac{\theta}{\theta r_{/R=0}}\right) \quad 21$$

where $\theta = T - T_f$ and $\theta_0 = T_0 - T_f$

3. Conclusion

Only the dimensionless parameters of fluid flow, convective, and conduction heat transfer were evaluated for the shaft kiln and further work on the method to study the radiative heat transfer and convective mass transfer is outstanding. The required pressure drop is below 100 kPa for fluid actual flow velocity less than 5 m/s. The low pressure requirements will allow for the evaluation of the heat and mass transfer at a wider range of fluid flow velocity. $B_i > 1$ indicates that the Mn ore residence time will play an important role in heat transfer. For a given column diameter and height the residence time will be specified at the point where the Mn ore at the kiln exit point is at 600 °C. The wall effect on the porosity variation in the radial direction of the packed bed need to be quantified before attempting to study the temperature distribution in the radial direction. Manually calculating the transport parameters for a high number of segments can be challenging and Python have been identified as a suitable tool to solving problems of this nature. When all the modes of heat transfer have been defined the heat transfer coefficients will be summed up to give an overall heat transfer coefficients for the axial and radial temperature gradients to complete the model. This will enable the tuning of the fluid flow rate per mass of solid materials in a shaft kiln of specific dimensions (bed diameter and bed height). The validation face of this work will be done both theoretically and through lab experiments. This will give indications in areas where the approach needs to be re-evaluated.

4. Acknowledgements

Sincere gratitude to Mintek and Vaal university of Technology for providing their facilities for this study and the PreMa project for the funding they put in to make this work possible. The PreMa project has received funding from the European Union's Horizon 2020 Research and Innovation Programme under Grant Agreement No 820561.

References

[1] Hockaday SAC, Dinter F, Harms TM (2018) Introducing solar thermal heat into minerals processing: A case study on replacing a diesel burner at a sinter plant. 8

[2] Gordon Y, Nell J, Yaroshenko Y (2018) Manganese Ore Thermal Treatment Prior to Smelting. KnE Eng 3(5): 71 - 86

[3] Yang J, Wang J, Bu S, Zeng M, Wang Q, Nakayama A (2011) Experimental analysis of forced convective heat transfer in novel structured packed beds of particles. Chem. Eng. Sci.71: 126 - 137

[4] Rickelt S (2011) Discrete element simulation and experimental validation of conductive and convective heat transfer in moving granular material. Ph.D. thesis. Bochum University. 173

[5] Vargas WL, McCarthy JJ (2001) Heat conduction in granular materials. AIChE. J 47(5): 1052 - 1059

[6] Van Antwerpen W, duToit CG, Gn PE, Rousseau D (2009) A review of correlations to model the packing structure and effective thermal conductivity in packed beds of mono-sizes spherical particles. Nucl. Eng Des 240: 1803 - 1818

[7] Bale S, Tiwari S, Sathe M, Berrouk AS, Nandakumar K, Joshi J (2018) Direct numerical simulation study of end effects and D/d ratio on mass transfer in packed beds. Int. J. Heat & Mass Transfer 127: 234 - 244

[8] Wen D, Ding Y (2006) Heat transfer of gas flow through a packed bed. Chem. Eng. Sci 61(11): 3532 - 3542

[9] Daizo H, Octave L (1992) Fluidisation Engineering. 2nd ed. Massachusetts Institute of Technology, USA

[10] Holman JP (2010) Heat Transfer, 10th ed. South Methodist University. McGrow-Hill, New York

[11] Geankoplis CJ (1993) Transport Process and Unit Operations, 3rd ed. Englewood Cliffs. PTR Prentice-Hall, New Jersey